I.Sofiya[1], Dr.D.Murugan[2]

Turkish Online Journal of Qualitative Inquiry (TOJQI)
Volume 12, Issue 8 July, 2021: 6425 – 6438

Research Article

Automatic detection of cell nuclei from H&E-stained based Marker-Controlled Segmented Histopathological Images

I.Sofiya[1], Dr.D.Murugan[2]
[1]Research Scholar, [2]Professor,
Department of CSE, Manonmaniam Sundaranar University,
Abishekapatti, Tirunelveli.
***Corresponding Author:** sofiya21193@gmail.com*

ABSTRACT

A computer-aided diagnosis system is the most important step for implementing an automated cell nuclei segmentation using cancer cells. Breast cancer is one of the world's major public health issues affecting women. It has two states: benign and malignant. Benign states are slow to develop, rarely spread to other parts of the body, and have well-defined borders. Malignant state, on the other hand, has a tendency to grow faster and is life threatening. Histopathological Images (HIs) are the gold standard for evaluating certain types of tumors for cancer diagnosis. Image segmentation techniques aim to identify and extract foreground objects in an image, resulting in individual segments. Image segmentation is fundamentally different from one type of image to the next because each has its own context and different geometrical properties, posing a challenge in designing a generic algorithmic procedure. In this paper, an effort is made to compare and study the efficiency of colour image segmentation using Fuzzy C-Means Clustering, segmentation using K-Means Clustering, Watershed Segmentation using Gradient, and proposed H&E Stained based Marker-Controlled towards tumor detection segmentation. The analysis concluded that the performance of Watershed Segmentation using Marker-Controlled produced better results than other techniques.

Keywords: Segmentation, Fuzzy C-Means, K-Means, Watershed with Gradient & Proposed Watershed with H&E based Marker-Controlled.

1. INTRODUCTION

Cancer is one of the primary cause of human mortality in the world. The utmost common cancer type in women is breast cancer. Timely detection and diagnosis plays a key role to control deaths due to breast cancer and it leads to the successful treatment. Presently, the screening techniques used for diagnosis of breast cancer are: mammography, ultrasound, fine needle aspirate, and biopsy. Mammography hardly detects cancer in dense breasts in adolescent women. It has 70-90% stated rate of cancer detection that concludes that the missed rate of breast cancer with mammography is 10-30% [1]. Histopathological images obtained from biopsy may influence how and at which stage the cancer is being diagnosed. Histopathological images allow early detection of tumor but there are difficulties with manually analysing these images. The current developments in digital pathology has the potential to reduce the workload of histopathologists by overcoming the subjective interpretation [2]. Furthermore, image segmentation for cell analysis to be precise generally requires great work effort. It is due to the huge variabilities caused because of dissimilar microscopes, inhomogeneous intensities of cells, type of cells, and stains. The complex data of cells and images is a major cause for problems in cell analysis [3]. To overcome these factors, various segmentation techniques exist in the literature

[4, 5]. Image segmentation is a process that is used to detect objects or boundaries in an image, which is distinguished between foreground and background pixels according to many characteristics. Several techniques have been recognized in literature to segment cells from neighboring tissues in histopathological images. The efforts to simplify segmentation techniques anticipated in literature fails frequently because these techniques work appropriately only for particular images.

Segmentation is a critical and settled exploration point in the field of image analysis and Computer vision. It is the most troublesome errand in image processing. Segmentation is the process of grouping the pixels that presents homogeneous characteristics, i.e. segmenting the image into various regions or objects. All consequent interpretation tasks, for instance, object recognition and classification depends vivaciously on the nature of the segmentation process.

The techniques based on pixel used for nuclear segmentation are the modest ones [6]. They depend upon the pixel value information such as texture, gray level or color. This is done either by using pixel classification or by automatic multi-thresholding using image histogram. Various thresholding techniques are used in which one or more thresholds must be determined to extract important objects from images [7-9]. Such type of techniques do not yield stable results as they have huge variabilities within image sets and they incline to work only on high-contrast images [6, 10]. Wang et al. involved thresholding technique to detect mitosis in histopathological images of breast [11, 12]. The limitations of thresholding technique in [12] was that it was not implemented using multiple layers of CNN model. Kowal et al. employed adaptive thresholding technique to segment histopathological images of breast cancer that further helped in differentiating the different type of tumors such as malignant and benign [13]. Singh and Filipczuk employed Adaptive thresholding technique to segment and further classify breast cancer Hematoxylin and Eosin (H&E) images [14-16]. Watershed algorithms and Active Contour Models (ACMs) are mostly used for segmentation of microscopic images [17, 18]. Qu et al. introduced an automatic computing system based on Marker Controlled Watershed that was used to extract all the morphological features in order to develop a classification model which could predict breast cancer [19].

Active contours are used for medical image segmentation, edge detection and object tracking [20]. Ali et al. introduced an Active Contour Model (ACM) based on region segmentation where nucleus and glandular structures were segmented [21-23]. Zarella et al. reported a scheme to segment nuclei from other parts of the cell using Otsu thresholding [24]. In literature number of research work has been done using fuzzy set and neutrosophic set for image segmentation [25, 26]. Various hybridised models have been presented in literature [27-29]. Vahadane et al. reported a technique to overcome the issue of over-segmentation and enhanced performance of watershed using Otsu thresholding technique [27]. Mouelhi et al. developed a segmentation technique combining an enhanced watershed technique and a new model of fuzzy active contour for cell images of breast cancer [28]. Husham et al. discussed another hybridized technique based on level set and Otsu thresholding for nuclei detection and segmentation [29].

2.1 RELATED WORKS

In the natural environment of the orchard, a segmentation method that works with varying illumination is yet to be demonstrated. The segmentation effect under the influence of alternating lighting and shadows remains to be verified. The segmentation process becomes easier when the difference between the fruit and the background is large. However, the interference of natural light and other factors in the orchard environment reduces this difference, and increases the difficulty in identification [30]. In this study, we propose a method to segment the apple image based on gray-centered RGB color space. In gray-centered RGB color space, this paper presents a novel color feature selection method which accounts for the influence of halation and shadow in apple images. By exploring both color features and local variation contents in apple images, we propose an efficient

patch-based segmentation algorithm that is a generalization of the K-means clustering algorithm. Extensive experiments prove the effectiveness and superiority of the proposed method.

The *k*-means algorithm is an unsupervised ML method for clustering that has been used for the segmentation of pixel regions. In the context of this review, it represents the core of fourteen segmentation methods. Fatakdawala et al. [31] proposed a methodology based on the expectation-maximization of the geodesic active contour for detecting lymphocyte nuclei, which can identify four structures: lymphocyte nuclei, stroma, cancer nuclei, and background. The process initiates with segmentation by a *k*-means algorithm, which clusters pixels of similar intensities, and afterward, such clusters are improved with an expectation-maximization algorithm. The contours are identified based on the magnetic interaction theory. After the definition of contours, an algorithm searches for contours' concavity, meaning nuclei are overlapping. The experiments were conducted using a breast cancer dataset. A multiscale segmentation with *k*-means is the subject of study of Roullier et al. [32].

This work uses the same idea of the pathologist to analyze a whole slide image (WSI). The segmentation starts at a lower magnification factor and finishes at a higher magnification, where it is easier to identify mitotic cells. The result of the clustering algorithm aims to identify regions of interest in each magnification. Rahmadwati et al. [33] employed the *k*-means algorithm to help classify HIs. Although the focus is not on the *k*-means but Gabor filters, this clustering method is essential in the segmentation process. Peng et al. [34] used *k*-means and principal component analysis (PCA) to split HIs into four types of structures: glandular lumen, stroma, epithelial-cell cytoplasm, and cell nuclei. Subsequently, morphological operations of closing and filling are performed. He et al. [35] used a mixture of local region-scalable fitting and *k*-means to segment cervix HIs. Fatima et al. [36] used *k*-means for segmentation followed by skeletonization and shock graphs to identify nuclei in the previously segmented image. If the shock graph provides a confidence value smaller than 0.5 for nucleus identification, the second attempt of identification is made using a multilayer perceptron (MLP). This hybrid approach achieves 92.5% of accuracy in nucleus identification. Mazo et al. [37] also used *k*-means to segment cardiac images in three classes: connective tissues, light areas, and epithelial tissue. A flooding algorithm processes light areas to merge its result with epithelial regions and improve the final result. Finally, the plurality rule was used to assign cells into flat, cubic, and cylindrical. This method achieved a sensitivity of 85%.

This work was extended in Mazo et al. [38]. Tosun et al. [39] proposed segmentation based on *k*-means that clusters all pixels into three categories (purple, pink, white), which are further divided into three subcategories. The object-level segmentation based on clustering achieved 94.89% of accuracy against 86.78% for pixel-level segmentation. Nativ et al. [40] presented a *k*-means clustering based on morphological features of lipid droplets previously segmented using active contours models. A decision tree (DT) was used to verify the rules that lead to the classes obtained by the clustering. The correlation with pathologist evaluations reached 97%. A two-step *k*-means is used by Shi et al. [41] to segment follicular lymphoma HI. The first step segments nuclei and other types of tissues into two clusters. The next step segments "another type tissue" area from the previous step into three classes (nuclei, cytoplasm, and extracellular spaces). The final step is a watershed algorithm to extract better contours of nuclei. The difference between manual segmentation and automated was around 1%. Brieu et al. [42] presented a segmentation approach based on *k*-means. The result of *k*-means segmentation is improved and simplified using a sequence of thresholds that attempt to preserve the form of objects. The key point of such a method is not the segmentation but nucleus detection. Shi et al. [43] used *k*-means to cluster pixels represented in the CIELAB color space using pixel neighborhood statistics. A thresholding step improves contours detection of fat droplets, and human specialists analyze morphological information related to the droplets to come up with a diagnosis.

Shi et al. [41] proposed a segmentation method that considers the local correlation of each pixel. A first clustering performed by a *k*-means algorithm generates a poorly segmented cytoplasm, and a second clustering that does not consider the nuclei identified by the first clustering is performed. Finally, a watershed transform is applied to complete the segmentation. Other clustering algorithms have also been used to segment HIs. The work proposed by Liu et al. [44] used the iterative self-organizing data analysis technique (ISODATA) to cluster cell images and create prototypes. Hafiane et al. [45] studied two strategies for initialization of clustering methods: geodesic active contours and multi-phase vector level sets. The last one proved to be more efficient when using spatial constraint fuzzy c-means, with accuracy values of 68.1% and 67.9% respectively, and *k*-means achieved 60.6% in this case. He et al. [46] presented segmentation based on Gaussian mixture models. Their methodology uses the stain color features (hematoxylin with blue color and eosin in pink and red) to apply two segmentation steps in the red channel and other channels subsequently. It does not present ground truth comparison, only visual results compared to *k*-means. [47] Presented a quasi-supervised approach based on nearest neighbors to cluster an unlabeled dataset based on itself and another labeled dataset. A comparison between the quasi-supervised approach and support vector machine (SVM) has shown that SVM presents a better performance, but it requires labeled data. Yang et al. [48] proposed a system for content recovery based on a three-step method that uses histogram features. The first two steps use dissimilarity measures of histograms to find candidate images. The last step uses mean shift clustering. The area under the curve (AUC) of the proposed method is 0.87, which is better than 0.84 achieved by the method based on local binary patterns (LBP) features. A mitotic cell detection system using a dictionary of cells is presented by Sirinukunwattana et al. [49]. A shrinkage/thresholding method groups intensity features represented by a sparse coding to create a dictionary. This method achieved 80.5% and 77.9% of F-score on Asperio and Hamatsu subsets of MITOS dataset, respectively. Huang [50] proposed a semi-supervised method based on exclusive component analysis (XCA) that uses the separation of stains to improve the performance. This method needs a small interaction of the user, who must provide a set of references from nuclei and from the cytoplasm. Finally, it is worth mentioning that unsupervised methods based on DL approaches have also been proposed for segmenting HIs. In this paper, we describe various pre-processing and segmentation methods which have been used in image analysis.

3. METHODOLOGY

The method begins with a colour deconvolution algorithm that divides the H&E-stained histopathology image into H&E channels. The hematoxylin channel is then subjected to morphological operations and thresholding techniques in order to determine the markers for use in nuclei segmentation with fuzzy c-means clustering, k-means clustering, watershed with gradients, and the proposed H&E-based marker-controlled watershed transform algorithm. Finally, the segmentation results are refined using the proposed H&E-based marker controlled watershed approach by minimising an objective function that estimates the number of overlapping nuclei in the segmented regions.

3.1 Dataset Description

The image dataset is made up of high-resolution (2040 1536 pixels), uncompressed, and annotated H&E stain images from the Bioimaging 2015 breast histology classification challenge [53]. All of the images are digitised under the same conditions, with a magnification of 200 and a pixel size of 0.42m 0.42m. Each image is labelled with one of four classes: I normal tissue, ii) benign lesion, iii) malignant in situ carcinoma, and iv) malignant invasive carcinoma The labelling was done by two pathologists who only provided a diagnostic based on the image contents without specifying the area of interest for the classification. Cases of disagreement between specialists were discarded. The challenge's goal is to provide an automatic classification of each input image.

The hematoxylin and eosin staining causes the nuclei and cytoplasm to appear purple and pinkish, respectively. The dataset is made up of an extended training set of 249 images and a separate test set of 20 images. The four classes in these datasets are balanced. The images were chosen so that the pathology classification could be determined objectively based on the image contents.

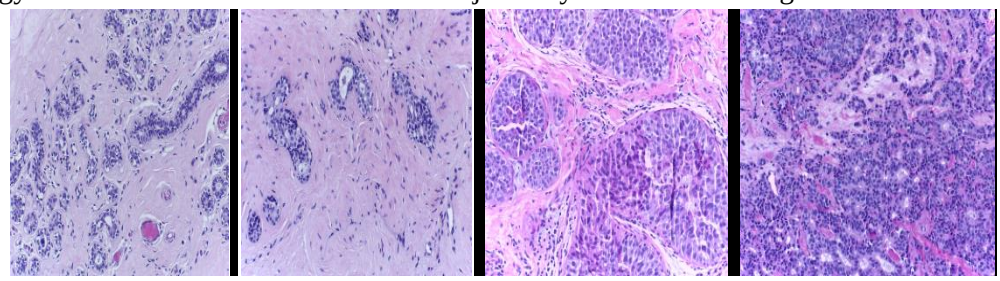

A B C D

Fig 1. Examples of microscopy image patches from the used dataset [53]. A normal tissue; **B** benign abnormality; **C** malignant in situ carcinoma; **D** malignant invasive carcinoma.

3.2Pre-processing

Image quality variations can have a significant impact on image segmentation. These variations are caused by a variety of factors, including inconsistent conditions during tissue slice preparation or image acquisition. Appropriate pre-processing methods, such as colour normalisation to minimise staining variations, spatial filtering to highlight major image structure, denoising to reduce image noise, and enhancement to optimise contrast between objects of interest and background, could all help to reduce variations to some extent.

3.3 Segmentation

Image segmentation is an important aspect of image processing. It becomes more important when dealing with medical images where pre- and post-surgery decisions are required for the purpose of initiating and hastening the recovery process. The need for maximum accuracy drives computer-aided detection of abnormal tissue growth. Manual segmentation of these abnormal tissues cannot be compared to today's high-speed computing machines, which allow us to visually observe the volume and location of unwanted tissues.

3.3.1 Segmentation Using Fuzzy C-Means Clustering

The fuzzy c-mean algorithm is a popular image segmentation algorithm that divides the image space into various cluster regions with similar pixel values. It's commonly used in image segmentation and pattern recognition. Fuzzy clustering is the best clustering method for medical image segmentation. The Fuzzy c-means (FCM) algorithm can be thought of as a fuzzy version of the k-means algorithm. It is a clustering algorithm that allows data items to have varying degrees of belonging to each cluster based on membership [54]. The algorithm is an iterative clustering method that finds the best c partition by minimising the weighted within group sum of squared error objective function.

3.3.2 Segmentation Using K-Means Clustering

K Means is a clustering algorithm. Clustering algorithms are unsupervised algorithms which mean that there is no labelled data available. It is used to identify different classes or clusters in the given data based on how similar the data is. Data points in the same group are more similar to other data points in that same group than those in other groups. K-means clustering is one of the most commonly used clustering algorithms. Here, k represents the number of clusters.

3.3.3 Watershed Segmentation Using Gradients

The preprocessing of a gray-scale image before using the Watershed transformation for segmentation can be done with the help of gradient magnitude. Dilation and erosion can be used in combination with image subtraction to obtain the Morphological Gradient image with the smoothened

image. The regions in an image are thickened and shrunk by dilation and erosion. Watershed Segmentation based on Morphological Gradient are introduced in Watershed Segmentation through opening and closing by reconstruction. Then reconstruction operators are in use to restructure gradient image in which a set of gradient pixels with high value are conserved and few gradient pixels with low value are detached. Thus improved algorithm using Gradients is applied to reconstruct image which eliminates over- segmentation but not completely. Although it holds the position of region contours clearly [51].

3.3.4 Proposed Watershed Segmentation Using H&E Stained Based Marker-Controlled

When Watershed Segmentation is applied directly to Gradient Magnitude images, it reveals the problem of over segmentation. The image to be segmented is converted to Grayscale in Marker-Controlled Watershed Segmentation. The image is then reconstructed by opening and closing it with a selection of markers based on foreground and background objects to determine the definite boundaries. It is dependable, efficient, and robust, and it produces results with low noise. It also works well with composite images. The main step in the proposed H&E Stained based marker-controlled method is to properly identify the markers, which include internal and external markers. The internal markers represent the cell nuclei that we are looking for, while the external markers represent the background regions that surround all of the cell nuclei. The external markers should be a connected component in the image. The steps to be followed includes

Step 1: Acquire Image

Step 2: Segment the H&E Image by Colour.

Step 3: Convert the colour image to gray colour.

Step 4: Pre-processing Image.

Step 5: Use the Gradient Magnitude as the Segmentation Function.

Step 6: Calculate foreground markers. These are the points that connect the pixels within each object.

Step 7: Calculate background markers. These are the pixels that do not belong to any object.

Step 8: Change the segmentation of function to have only edge values at the foreground and background markers

Step 9: Watershed transform of gradient image results in over segmentation

Step 10: Read the watershed transformed gradient image and applying Closing and Opening function by Reconstruction**.**

Step 12: Regional Maxima of gradient magnitude.

Step 13: Compute the Watershed Transform using Segmentation Function.

Step 14: Segment the Nuclei.

Step 15: Visualize the Result.

Once the markers have been determined, the watershed transform can locate the peaks or watersheds between the internal and external markers using the magnitude gradient hematoxylin image. To smooth the boundary, the morphological opening operation is used, which consists of morphological erosion followed by a dilation operation. For the morphological opening, a disk-shaped structuring element with radius 3 is used, which smoothes the boundary while also removing small protrusions. The distance transform algorithm is first applied to the smoothed binary image to identify the internal markers referring to cell nuclei. When the watershed transform technique is used on the modified gradient hematoxylin image, the over segmentation problem is reduced. A H&E-stained image labelled with markers (internal and external markers) and the segmentation result from the marker-controlled watershed transform algorithm.

4. EXPERMENTAL RESULTS

The implemented methods are experimented on histopathaology images which are downloaded from various sources of online. The evaluation of experimental results is carried out through subjective studies. The results of the methods nuclei detection are shown in the figure 1 to figure 4 and the analysis of the performance metrics shown in table 1 to 4.

4.1 Segmentation using Fuzzy C-Means Clustering

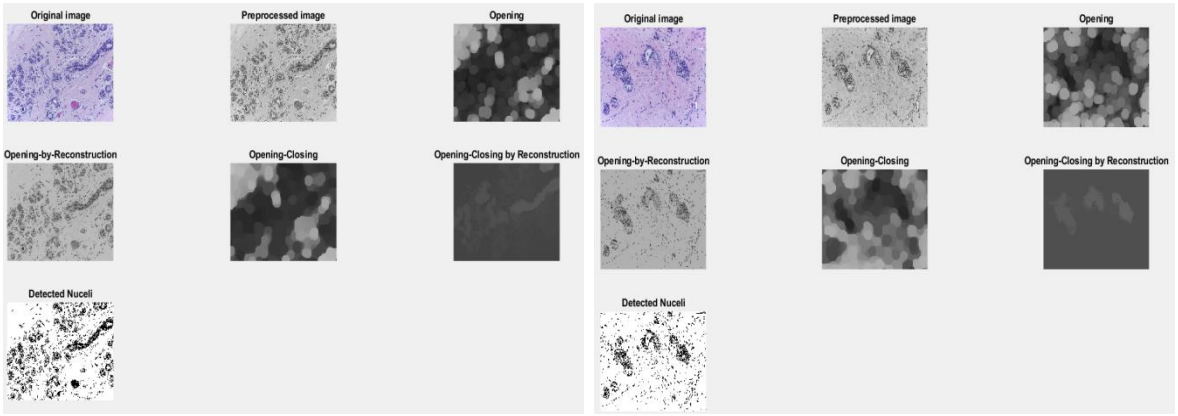

a) Normal **b) Benign**

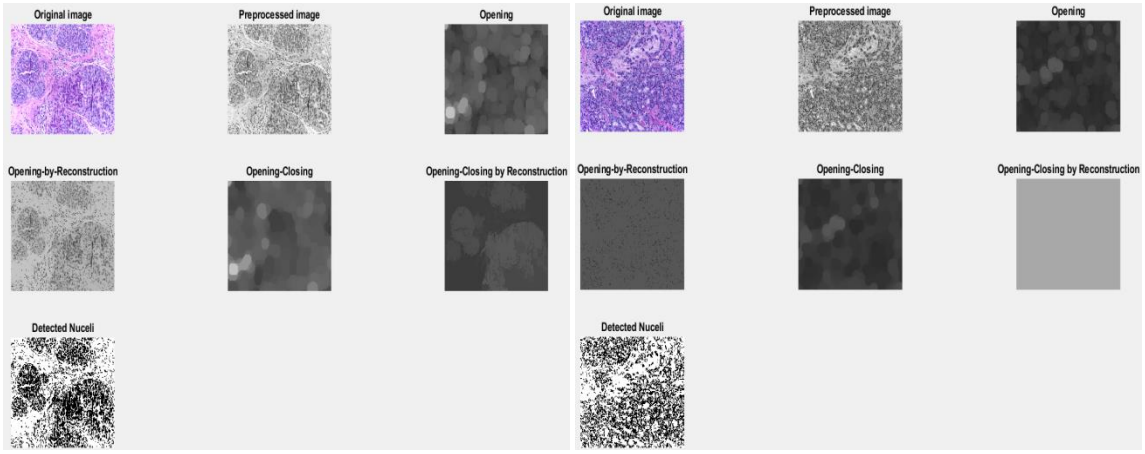

c) Malignant In Situ Carcinoma **d) Malignant Invasive Carcinoma**

Fig. 1: Segmentation Using Fuzzy C-Means Clustering.

Table 1. Performance Metrics of the BreakHis dataset Using Fuzzy C-Means Clustering

	Accuracy	Sensitivity	Specificity	PPV	NPV	F-Measure
Normal	95.01	98.65	71.43	94.29	97.68	83.34
Benign	93.56	97.89	75.57	97.36	98.25	86.04
Malignant In Situ	75.58	99.35	36.10	71.67	99.13	53.05
Malignant Invasive	92.68	98.58	88.79	93.45	98.57	94.06

4.2 Segmentation using K-Means Clustering

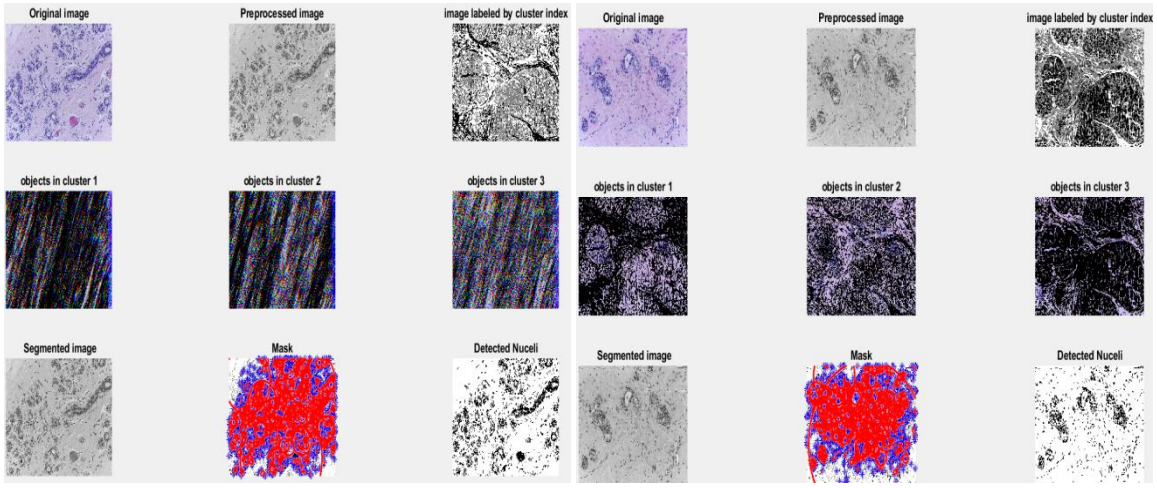

a) Normal **b) Benign**

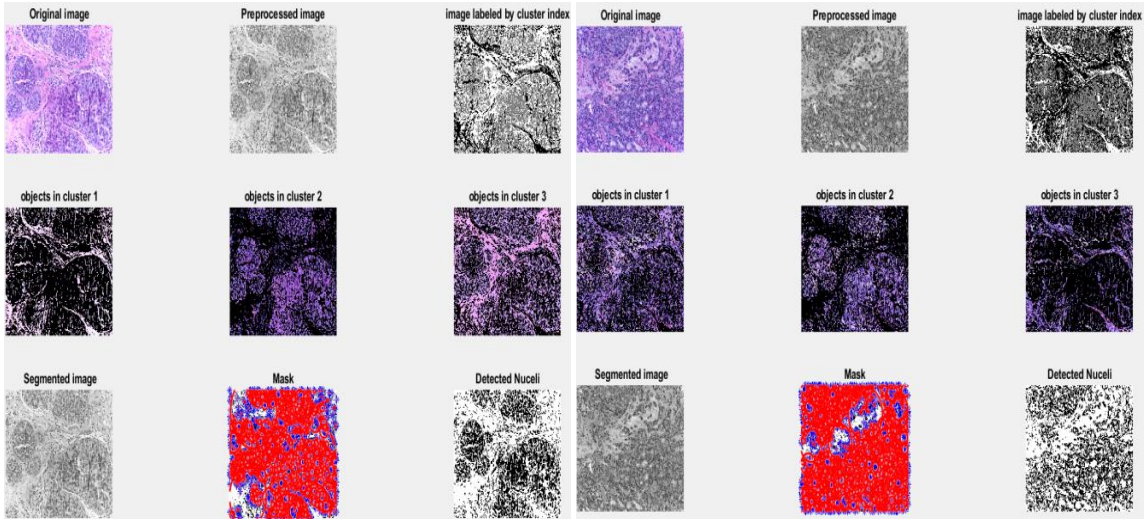

c) Malignant In Situ Carcinoma **d) Malignant Invasive Carcinoma**

Fig. 2: Segmentation Using K-Means Clustering.

Table 2. Performance Metrics of the BreakHis dataset Using K-Means Clustering

	Accuracy	Sensitivity	Specificity	PPV	NPV	F-Measure
Normal	93.01	96.35	71.43	94.29	95.02	83.34
Benign	92.73	97.55	85.69	83.81	76.90	98.76
Malignant In Situ	76.39	99.20	36.88	72.61	91.65	53.89
Malignant Invasive	91.68	93.45	86.69	90.58	88.79	96.61

4.3 Watershed Segmentation using Gradients

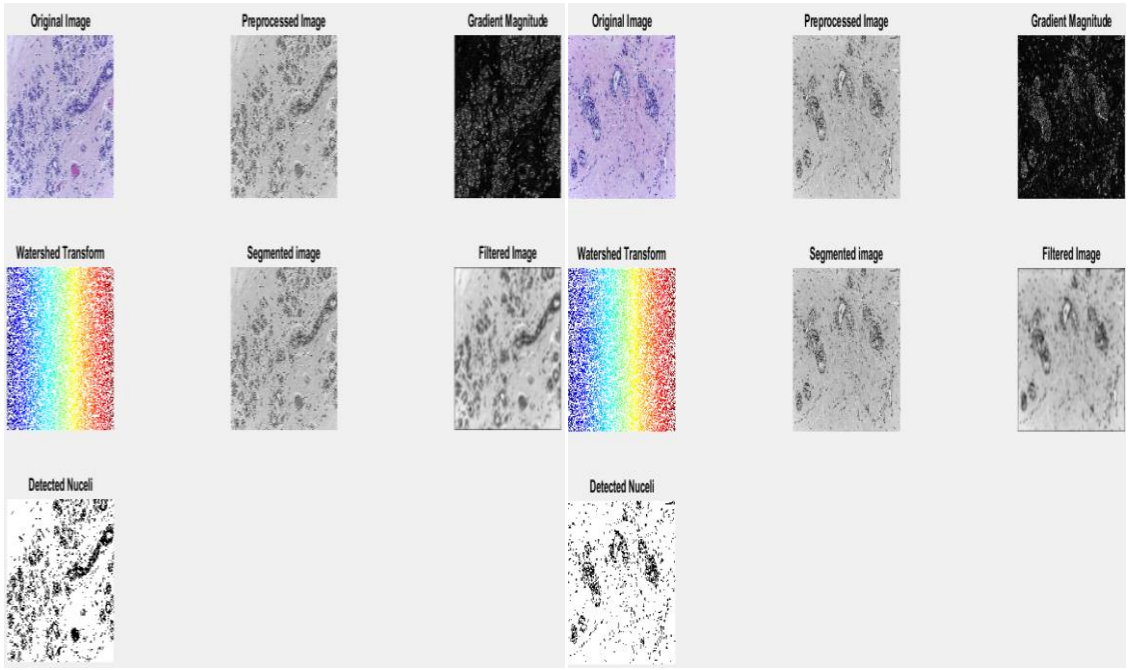

a) Normal **b) Benign**

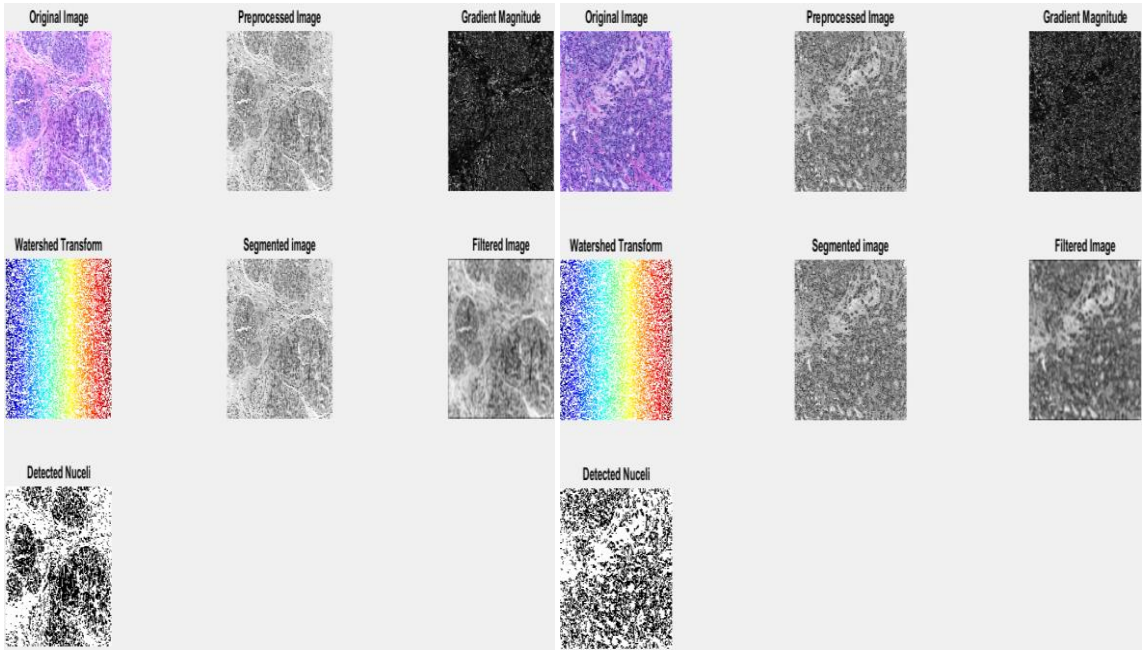

c) Malignant In Situ Carcinoma **d) Malignant Invasive Carcinoma**

Fig. 3: Segmentation Using Watershed with Gradients.

Table 3. Performance Metrics of the BreakHis dataset Using Watershed with Gradients

	Accuracy	Sensitivity	Specificity	PPV	NPV	F-Measure
Normal	94.86	98.25	72.53	95.29	98.11	84.64
Benign	95.68	96.25	94.56	99.30	80.30	89.26
Malignant In Situ	80.39	97.52	69.12	85.35	99.01	65.86
Malignant Invasive	95.36	91.55	96.25	98.54	89.46	90.25

4.4 Proposed Watershed Segmentation Using H&E Stained Based Marker-Controlled

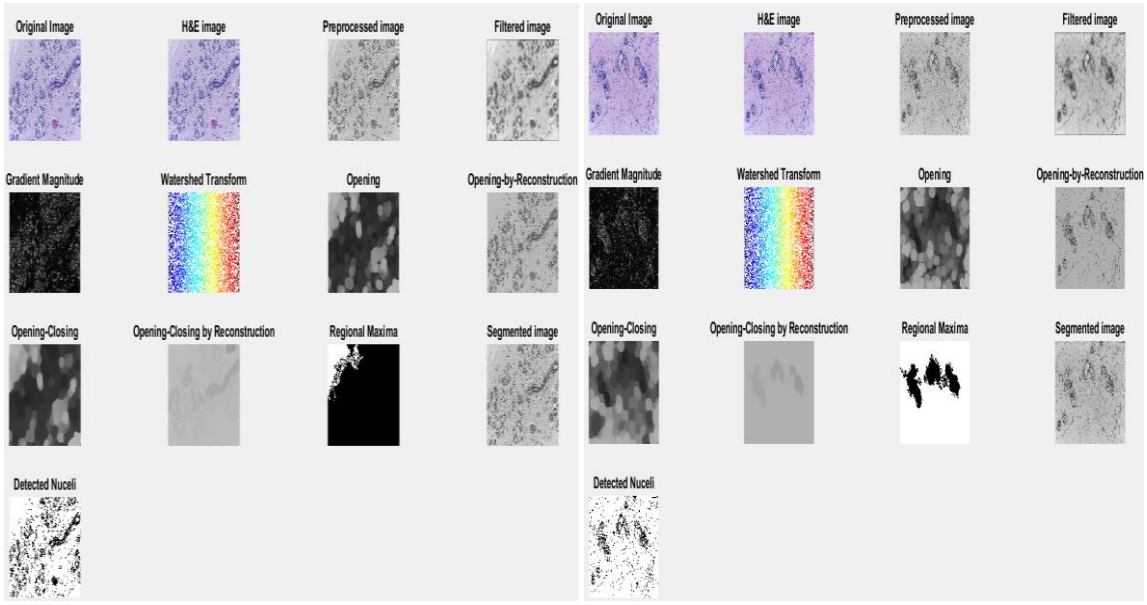

a) Normal **b) Benign**

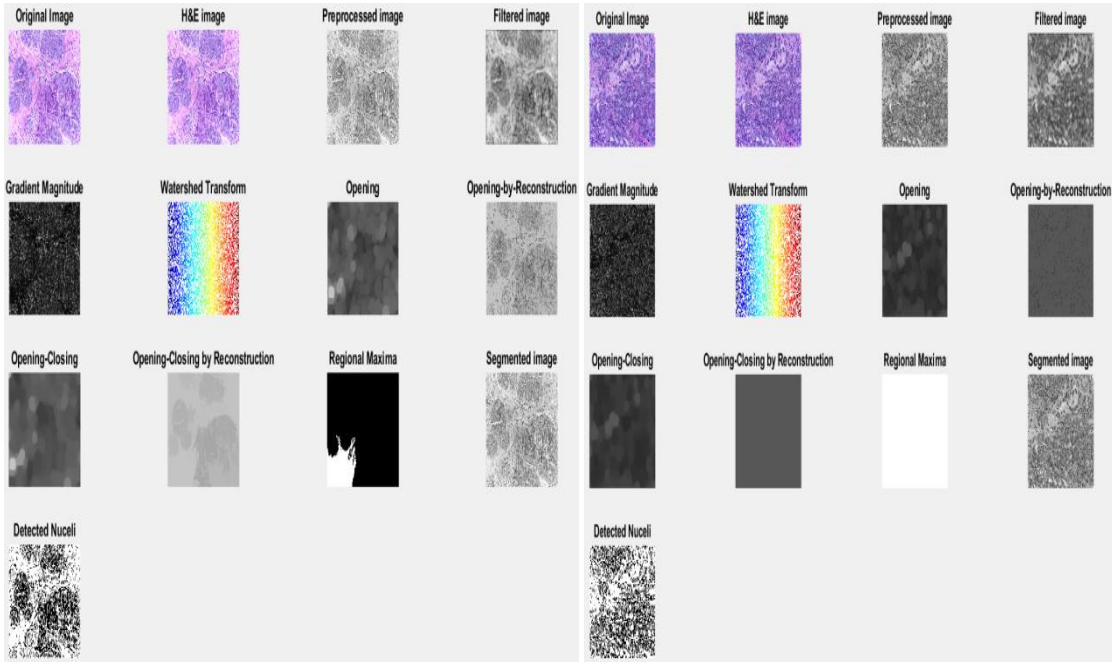

c) Malignant In Situ Carcinoma **d) Malignant Invasive Carcinoma**

Fig. 4: Proposed Segmentation Using H&E based Watershed.

Table 4. Performance Metrics of the BreakHis dataset Using Proposed Segmentation Using H&E based Watershed

	Accuracy	Sensitivity	Specficity	PPV	NPV	F-Measure
Normal	98.58	98.27	85.21	96.58	98.25	86.37
Benign	97.68	96.79	98.44	99.38	80.95	89.26
Malignant In Situ	89.39	99.69	69.12	85.35	99.08	65.86
Malignant Invasive	98.36	91.55	97.25	93.64	89.46	90.25

5. CONLCUSION

Image segmentation is the first step in the image processing and analysis process. Image segmentation divides the image into multiple parts, resulting in a significant difference between the image of the object and the background. In this paper, an effective and automatic computer-aided technique for pre-processing and segmentation is proposed and used. It describes an unsupervised method for segmenting nuclei in breast cancer biopsy images. The method is automatic and computationally efficient, requiring only a few parameters to be defined. An examination of a set of images with a variety of tissue appearances revealed that a large number of nuclei are segmented with high accuracy. Our experimental results show that the proposed watershed using H&E-based marker-controller nuclei extraction approach can achieve good segmentation results and achieve better performance in terms of segmentation accuracy and nuclei separation when compared to other nuclei extraction algorithms. The analysis concluded that the performance of the proposed watershed segmentation using H&E-based Marker Controlled yielded better results than other techniques.

REFERENCES

1. Siegel, R. L., Miller, K. D., & Jemal, A. (2016). Cancer statistics, 2016. CA: "A Cancer Journal for Clinicians", 66(1), 7-30.
2. Demir, C., & Yener, B. (2005). Automated cancer diagnosis based on histopathological images: a systematic survey. Rensselaer Polytechnic Institute, Technical Reports, 1-16.
3. Pan, X., Li, L., Yang, H., Liu, Z., Yang, J., Zhao, L., & Fan, Y. (2017). Accurate segmentation of nuclei in pathological images via sparse reconstruction and deep convolutional networks. Neurocomputing, 229, 88-99.
4. Xian, M., Zhang, Y., Cheng, H. D., Xu, F., Zhang, B., & Ding, J. (2018). Automatic breast ultrasound image segmentation: A survey. Pattern Recognition, 79, 340-355.
5. Huang, Q., Luo, Y., & Zhang, Q. (2017). Breast ultrasound image segmentation: a survey. International Journal of Computer Assisted Radiology and Surgery, 12(3), 493-507.
6. Di Cataldo, S., Ficarra, E., & Macii, E. (2012). Computer-aided techniques for chromogenic immunohistochemistry: status and directions. Computers in Biology and Medicine, 42(10), 1012-1025.
7. He, L., Long, L. R., Antani, S., & Thoma, G. R. (2012). Histology image analysis for carcinoma detection and grading. Computer Methods and Programs in Biomedicine, 107(3), 538-556.
8. Kim, Y. J., Romeike, B. F. M., Uszkoreit, J., & Feiden, W. (2006). Automated nuclear segmentation in the determination of the Ki-67 labeling index in meningiomas. Clinical Neuropathology, 25(2).
9. Loukas, C. G., & Linney, A. (2004). A survey on histological image analysis-based assessment of three major biological factors influencing radiotherapy: proliferation, hypoxia and vasculature. Computer Methods and Programs in Biomedicine, 74(3), 183-199.
10. Gurcan, M. N., Boucheron, L., Can, A., Madabhushi, A., Rajpoot, N., & Yener, B. (2009). Histopathological image analysis: a review. IEEE Reviews in Biomedical Engineering, 2, 147.
11. Wang, H., Roa, A. C., Basavanhally, A. N., Gilmore, H. L., Shih, N., Feldman, M., & Madabhushi, A. (2014). Mitosis detection in breast cancer pathology images by combining handcrafted and convolutional neural network features. Journal of Medical Imaging, 1(3), 1-8.
12. Wang, H., Roa, A. C., Basavanhally, A., Gilmore, H., Shih, N., Feldman, M., & Madabhushi, A. (2014). Cascaded ensemble of convolutional neural networks and handcrafted features for

mitosis detection. International Society for Optics and Photonics, In Medical Imaging, 9041, 1-10.
13. Kowal, M., Filipczuk, P., Obuchowicz, A., & Korbicz, J. (2011). Computer-aided diagnosis of breast cancer using Gaussian mixture cytological image segmentation. Journal of Medical Informatics and Technologies, 17.
14. Singh, S. (2012). Cancer cells detection and classification in biopsy image. International Journal of Engineering Science and Technology (IJEST). (38)3, 15-21.
15. Filipczuk, P., Kowal, M., & Obuchowicz, A. (2012). Breast fibroadenoma automatic detection using k-means based hybrid segmentation method. IEEE 9th International Symposium on Biomedical Imaging (ISBI), 1623-1626.
16. Kowal, M., Filipczuk, P., Obuchowicz, A., Korbicz, J., & Monczak, R. (2013). Computer-aided diagnosis of breast cancer based on fine needle biopsy microscopic images. Computers in Biology and Medicine, 43(10), 1563-1572.
17. Veta, M., Huisman, A., Viergever, M. A., van Diest, P. J., & Pluim, J. P. (2011). Marker-controlled watershed segmentation of nuclei in H&E stained breast cancer biopsy images. IEEE International Symposium on Biomedical Imaging, 618-621.
18. Veta, M., Van Diest, P. J., Kornegoor, R., Huisman, A., Viergever, M. A., & Pluim, J. P. (2013). Automatic nuclei segmentation in H&E stained breast cancer histopathology images. PloS one, 8(7), e70221.
19. Qu, A., Chen, J., Wang, L., Yuan, J., Yang, F., Xiang, Q., & Li, Y. (2014). Two-step segmentation of Hematoxylin-Eosin stained histopathological images for prognosis of breast cancer. IEEE.IEEE International Conference on Bioinformatics and Biomedicine (BIBM), 218-223.
20. Kass, M., Witkin, A., & Terzopoulos, D. (1988). Snakes: Active contour models. International Journal of Computer Vision, 1(4), 321-331.
21. Ali, S., & Madabhushi, A. (2011). Segmenting multiple overlapping objects via a hybrid active contour model incorporating shape priors: applications to digital pathology. Medical Imaging: Image Processing, 7962, 1-13.
22. Ali, S., & Madabhushi, A. (2011). Active contour for overlap resolution using watershed based initialization (ACOReW): Applications to histopathology. IEEE International Symposium on Biomedical Imaging: From Nano to Macro, 614-617.
23. Ali, S., & Madabhushi, A. (2012). An integrated region-, boundary-, shape-based active contour for multiple object overlap resolution in histological imagery. IEEE Transactions on Medical Imaging, 31(7), 1448-1460.
24. Zarella, M. D., Garcia, F. U., & Breen, D. E. (2017). A template matching model for nuclear segmentation in digital images of h&e stained slides. ACM 9th International Conference on Bioinformatics and Biomedical Technology, 11-15.
25. Koundal, D., Gupta, S., & Singh, S. (2016). Applications of Neutrosophic Sets in Medical Image Denoising and Segmentation. Infinite Study New Trends in Neutrosophic Theory and Applications, 257-275.
26. Koundal, D. (2017). Texture-based image segmentation using neutrosophic clustering. IET Image Processing, 11(8), 640-5.
27. Vahadane, A., & Sethi, A. (2013). Towards generalized nuclear segmentation in histological images. IEEE 13th International Conference on Bioinformatics and Bioengineering (BIBE), 1-4.
28. Mouelhi, A., Sayadi, M., & Fnaiech, F. (2013). Hybrid segmentation of breast cancer cell images using a new fuzzy active contour model and an enhanced watershed method. IEEE

International Conference on Control, Decision and Information Technologies (CoDIT), 382-387.

29. Husham, A., Hazim Alkawaz, M., Saba, T., Rehman, A., & Saleh Alghamdi, J. (2016). Automated nuclei segmentation of malignant using level sets. Microscopy Research and Technique, 79(10), 993- 997.
30. Vandenbroucke N, Macaire L, Postaire J-G. Color image segmentation by pixel classification in an adapted hybrid color space. Application to soccer image analysis. Computer Vision and Image Understanding. 2003;90(2):190–216
31. Fatakdawala, H.; Xu, J.; Basavanhally, A.; Bhanot, G.; Ganesan, S.; Feldman, M.; Tomaszewski, J.E.; Madabhushi, A. ExpectationMaximization-Driven Geodesic Active Contour With Overlap Resolution (EMaGACOR): Application to Lymphocyte Segmentation on Breast Cancer Histopathology. IEEE Trans. Biomed. Eng. 2010, 57, 1676–1689.
32. Roullier, V.; Lézoray, O.; Ta, V.T.; Elmoataz, A. Multi-resolution graph-based analysis of histopathological whole slide images: Application to mitotic cell extraction and visualization. Comput. Med. Imaging Graph. 2011, 35, 603–615.
33. Rahmadwati, Naghdy, G.; Ros, M.; Todd, C.; Norahmawati, E. Cervical Cancer Classification Using Gabor Filters. In Proceedings of the IEEE 1st International Conference on Healthcare Informatics, Imaging and Systems Biology, San Jose, CA, USA, 26–29 July 2011; pp. 48–52.
34. Peng, Y.; Jiang, Y.; Eisengart, L.; Healy, M.A.; Straus, F.H.; Yang, X.J. Segmentation of prostatic glands in histology images. In Proceedings of the IEEE International Symposium on Biomedical Imaging: From Nano to Macro, Chicago, IL, USA, 30 March–2 April 2011; pp. 2091–2094.
35. He, L.; Long, L.R.; Antani, S.; Thoma, G.R. Multiphase Level Set Model with Local K-means Energy for Histology Image Segmentation. In Proceedings of the IEEE 1st International Conference on Healthcare Informatics, Imaging and Systems Biology, San Jose, CA, USA, 26-29 July 2011, pp. 32–39.
36. Fatima, K.; Arooj, A.; Majeed, H. A New Texture and Shape Based Technique for Improving Meningioma Classification. Microsc. Res. Tech. 2014, 77, 862–873.
37. Mazo, C.; Trujillo, M.; Alegre, E.; Salazar, L. Automatic recognition of fundamental tissues on histology images of the human cardiovascular system. Micron 2016, 89, 1–8.
38. Mazo, C.; Alegre, E.; Trujillo, M. Classification of cardiovascular tissues using LBP based descriptors and a cascade SVM. Comput. Methods Programs Biomed. 2017, 147, 1–10.
39. Tosun, A.B.; Kandemir, M.; Sokmensuer, C.; Gunduz-Demir, C. Object-oriented texture analysis for the unsupervised segmentation of biopsy images for cancer detection. Pattern Recognit. 2009, 42, 1104–1112.
40. Nativ, N.I.; Chen, A.I.; Yarmush, G.; Henry, S.D.; Lefkowitch, J.H.; Klein, K.M.; Maguire, T.J.; Schloss, R.; Guarrera, J.V.; Berthiaume, F.; et al. Automated image analysis method for detecting and quantifying macrovesicular steatosis in hematoxylin and eosin-stained histology images of human livers. Liver Transplant. 2014, 20, 228–236.
41. Shi, P.; Zhong, J.; Huang, R.; Lin, J. Automated quantitative image analysis of hematoxylin-eosin staining slides in lymphoma based on hierarchical Kmeans clustering. In Proceedings of the 8th International Conference on Information Technology in Medicine and Education, Fuzhou, China, 23–25 December 2016; pp. 99–104.
42. Brieu, N.; Pauly, O.; Zimmermann, J.; Binnig, G.; Schmidt, G. Slide-Specific Models for Segmentation of Differently Stained Digital Histopathology Whole Slide Images. In

Proceedings of the SPIE Medical Imaging 2016: Image Processing, San Diego, CA, USA, 21 March 2016; Volume 9784.

43. Shi, P.; Chen, J.; Lin, J.; Zhang, L. High-throughput fat quantifications of hematoxylin-eosin stained liver histopathological images based on pixel-wise clustering. Sci. China Inf. Sci. 2017, 60.
44. Liu, B.; Liu, Y.; Zhang, J.; Zeng, Y.; Wang, W. Application of the synergetic algorithm on the classification of lymph tissue cells.Comput. Biol. Med. 2008, 38, 650–658.
45. Hafiane, A.; Bunyak, F.; Palaniappan, K. Evaluation of level set-based histology image segmentation using geometric region criteria. In Proceedings of the IEEE International Symposium on Biomedical Imaging: From Nano to Macro, Boston, MA, USA, 28 June–1 July 2009; pp. 1–4.
46. He, L.; Long, L.R.; Antani, S.; Thoma, G.R. Local and global Gaussian mixture models for hematoxylin and eosin stained histology image segmentation. In Proceedings of the 10th International Conference on Hybrid Intelligent Systems, Atlanta, GA, USA, 23–25 August 2010; pp. 223–228.
47. Onder, D.; Sarioglu, S.; Karacali, B. Automated labelling of cancer textures in colorectal histopathology slides using quasisupervised learning. Micron 2013, 47, 33–42.
48. Yang, L.; Qi, X.; Xing, F.; Kurc, T.; Saltz, J.; Foran, D.J. Parallel content-based sub-image retrieval using hierarchical searching.Bioinformatics 2014, 30, 996–1002.
49. Sirinukunwattana, K.; Khan, A.M.; Rajpoot, N.M. Cell words: Modelling the visual appearance of cells in histopathology images. Comput. Med. Imaging Graph. 2015, 42, 16–24.
50. Huang, C.H. Semi-supervised color decomposition for histopathological images using exclusive component analysis. In Proceedings of the IEEE 25th International Workshop on Machine Learning for Signal Processing (MLSP), Boston, MA, USA, 17–20 September 2015.
51. Baoan Han,"Watershed Segmentation Algorithm Based on Morphological Gradient Reconstruction" ,IJCE, IEEE 11 June 2015,pp 533-536
52. S.Madhumitha and M. Manikandan ,"Quantitative Analysis of Marker-based Watershed Image Segmentation", current science, vol. 114, no. 5, 10 March 2018,pp 1007-1013
53. Pêgo A, Aguiar P. Bioimaging 2015; 2015. Available from: http://www.bioimaging2015.ineb.up.pt/dataset.html.
54. Hind Rustum Mohammed, "Improved Fuzzy C-Mean Algorithm for Image Segmentation", International Journal of Advanced Research in Artificial Intelligence (IJARAI), Vol. 5, No.6, 2016.